

We are IntechOpen, the world's leading publisher of Open Access books Built by scientists, for scientists

6,900

Open access books available

186,000

International authors and editors

200M

Downloads

Our authors are among the

154

Countries delivered to

TOP 1%

most cited scientists

12.2%

Contributors from top 500 universities



WEB OF SCIENCE™

Selection of our books indexed in the Book Citation Index
in Web of Science™ Core Collection (BKCI)

Interested in publishing with us?
Contact book.department@intechopen.com

Numbers displayed above are based on latest data collected.
For more information visit www.intechopen.com



Computerized Image Analysis of Mammographic Microcalcifications: Diagnosis and Prognosis

Anna N. Karahaliou, Nikolaos S. Arikidis, Spyros G. Skiadopoulos,
George S. Panayiotakis and Lena I. Costaridou
*Department of Medical Physics, Faculty of Medicine,
University of Patras, Rio,
Greece*

1. Introduction

Breast cancer is the second leading cause of cancer deaths in women today (after lung cancer) and is the most frequently diagnosed cancer among women, excluding skin cancers. According to the American Cancer Society, an estimated of 230,480 new cancer cases are expected to be diagnosed in 2011; about 2,140 new cases are expected in men. In addition to invasive breast cancer, 57,650 new cases of in situ breast cancer are expected to occur among women in 2011. Of these, approximately 85% will be ductal carcinoma in situ (DCIS). An estimated 39,970 breast cancer deaths (39,520 women, 450 men) are expected in 2011. Death rates for breast cancer have steadily decreased in women since 1990, with larger decreases in women younger than 50 (a decrease of 3.2% per year) than in those 50 and older (2.0% per year), representing progress in both earlier detection and improved treatment.

Breast imaging has a key role in the early detection of breast cancer, which in conjunction with increased public awareness (prompting for monthly self-breast examination and annual examination by physician) yields the reduction in mortality from breast cancer.

Screen-film (SF) mammography is currently the most effective imaging modality for the early detection of breast cancer, challenged however by the presence of dense breast parenchyma. Furthermore, radiologist accuracy in diagnostic task (discrimination of malignant from benign lesions) is relatively low and is also differentiated with respect to lesion type (masses versus microcalcifications) (Cole et al., 2003). Despite the advantages offered by digital mammography the diagnosis of indeterminate lesions is still a challenging task. Breast ultrasound and Dynamic Contrast Enhanced Magnetic Resonance Imaging (DCE-MRI) are significant adjuncts to mammography providing additional diagnostic information by exploiting 3D structural and functional tissue properties related to lesion angiogenesis.

Computer-Aided Detection (CADe) and Computer-Aided Diagnosis (CADx) schemes have been proposed across breast imaging modalities to improve radiologist performance in detection and diagnosis tasks (Bassett, 2000; Cheng et al., 2003; Sampat et al., 2005; Chan et

al., 2005; Giger et al., 2008; Costaridou et al., 2008; Elter & Horsch, 2009). These schemes also aim to reduce intra- and inter-observer variability by quantifying information that the human observer can perceive but in an objective and reproducible way (“mimic the human eye”), or to further quantify any information that may not be readily perceived by human eyes. The challenges of the CADx approaches are differentiated across breast imaging modalities and lesion types.

The American College of Radiology (ACR) Breast Imaging Reporting and Data System (BI-RADS) lexicon (ACR BIRADS 2003) defines masses, microcalcification (MC) clusters, architectural distortion and bilateral asymmetry as the major breast cancer signs in X-ray mammography. A mass is a space occupying lesion seen at least in two different mammographic projections. If a mass is seen only in a single projection is called asymmetric density. When a focal area of breast tissue appears distorted with spiculations radiating from a common point and focal retraction at the edge of the parenchyma, while no central mass is definable, it is called architectural distortion.

Calcifications are small deposits of calcium within the breast tissue and as masses are associated with both malignant and benign underlying biological processes (Kopans, 2007). Calcifications appear as high Signal-to-noise-ratio (SNR) bright structures, due to the high attenuation coefficient of calcium (higher than other breast constituents such as water, fat and glandular tissue). Calcifications can be large (>1mm) referred to as macro-calcifications and are commonly associated with benign conditions. MCs are tiny deposits of calcium in the breast with size ranging from 0.1mm to 1mm. A number of MCs grouped together is termed as a cluster and it may be a strong indication of cancer. A cluster is defined as at least three MCs within a 1 cm² area. Benign MCs are usually larger and coarser with round and smooth contours. Malignant MCs tend to be numerous, clustered, small, varying in size and shape, angular, irregularly shaped and branching in orientation.

In x-ray mammography, the automated interpretation of MCs is an open issue and more difficult than the corresponding task for masses (Cheng et al., 2003; Sampat et al., 2005). Difficulty in automated MCs interpretation is attributed to MCs fuzzy nature (varying size and shape), low contrast and low distinguishability from their surroundings (Cheng et al., 2003) rendering the accurate segmentation of MCs a challenging task. CADx schemes for MC clusters can be categorized into two major approaches: morphology-based and texture-based approaches. The morphology-based CADx schemes are highly dependent on the robustness of the employed segmentation algorithm. Texture-based CADx schemes assume that the presence of MCs alters the texture of the background tissue that MCs are embedded in; focused on extracting texture features from Regions of Interest (ROI) containing the cluster, these approaches do not depend on the robustness of a segmentation algorithm (i.e. the segmentation step is omitted). Since it is the breast tissue surrounding MCs that is subjected to histopathological analysis, to derive a malignant or a benign outcome, mammographic image texture analysis seems a more natural choice, while the bias induced by the presence of MCs on the texture pattern of the ROI being analyzed should also be considered (Thiele et al., 1996).

The following sections provide the current state-of-the-art approaches towards computer-aided diagnosis of MC clusters. Specifically, morphology-based and texture-based approaches are reviewed and an application paradigm focusing on their inter-comparison is provided.

2. Computer-aided detection and diagnosis of breast lesions in x-ray mammography

While SF mammography is currently the most effective breast imaging modality for the early detection of breast cancer (detection of breast abnormalities/lesions), its specificity in differentiating malignant from benign lesions is relatively low resulting in a high number of unnecessary biopsies.

Digital mammography allows the separation of image acquisition, processing, and display and represents a solution to many of the inherent limitations of SF mammography (Pissano, 2000). The digital detector has a linear response to x-ray intensity, in contrast to the sigmoidal response of screen-film systems. As a result, use of a digital detector provides a broader dynamic range of densities and higher contrast resolution. Through image processing, display parameters may be chosen independently from image acquisition factors. Small differences in attenuation between normal and abnormal breast tissue can be amplified, rendering digital mammography most suitable for screening of dense breast.

Despite the advantages offered by digital mammography, the radiologic interpretation of MCs still remains a major issue and is more challenging than the interpretation of breast masses. Studies have shown that the performance of radiologists in interpreting breast lesions is highly dependent on lesion type (masses vs. MCs) even with the use of image post-processing techniques (Cole et al., 2003). Specifically, it has been shown that radiologist performance in MCs interpretation is reduced as compared to masses interpretation, independent of the post-processing method used (Cole et al., 2003). Furthermore, inter- and intra-observer variability is higher in MCs interpretation as compared to masses interpretation (Skaane et al., 2008), and is also similar to observer variability in SF mammography (Baker et al., 1996; Skaane et al., 2008).

CADe and CADx schemes have a key role in detection and diagnosis of breast lesions aiming to improve radiologist performance, reduce observer variability and quantify lesion properties (Bassett, 2000; Cheng et al., 2003; Sampat et al., 2005; Chan et al., 2005; Costaridou et al., 2008; Costaridou, 2011). They were originally proposed and applied on digitized images with proven benefits, but as being better suited to digitally acquired images they are expected to cast further insights towards breast cancer detection and management. These systems act only as “second readers” and the final decision is made by the radiologist. The term “CADe/x” refers to formulating the clinical detection or diagnosis problem into the context of quantitative image feature extraction and pattern classification with the goal of solving it automatically (Duncan & Ayache, 2000).

CADe schemes have been developed to improve radiologists’ performance in detecting breast lesions, by identifying suspicious regions of masses and MC clusters in an image (i.e. by placing prompts over areas of concern). The input to a CADe scheme is an image and the output is a location of a possible abnormality. Recent CADe schemes also provide the lesion boundary. CADx schemes in breast imaging aim to assist radiologists in the diagnostic task of lesion characterization (malignancy vs. benignity), thus affecting patient management (follow-up vs. biopsy). The input to a CADx scheme is a ROI indicating a breast lesion/abnormality. The output of a CADx scheme is a probability of malignancy for the

lesion considered. Both CADe and CADx schemes share similar processing stages, such as segmentation, feature extraction and classification adjusted however to the specific task at hand. Figure 1 depicts the typical architecture of a CADe and a CADx scheme.

The high performances achieved by CADe schemes for breast lesions in x-ray mammography have led to their incorporation in commercially available FDA approved systems. These systems have shown to improve the performance of radiologists in detecting breast lesions, however, the high rate of false positives reported by some studies arise controversies concerning their exact impact on radiologist interpretation (Gur et al., 2004, Fenton et al., 2007). On the other hand, the development of commercially available CADx systems is still ongoing (Sampat et al., 2005).

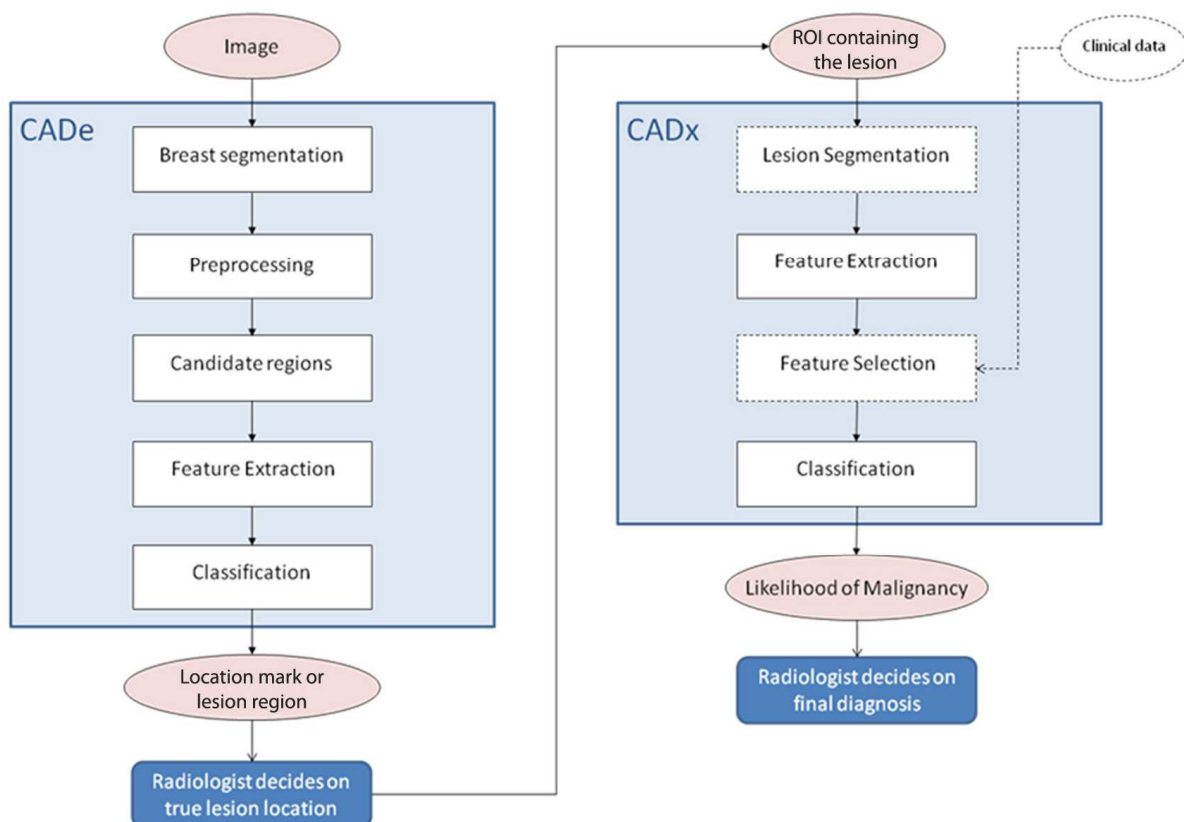


Fig. 1. Flowchart depicting the typical architecture of a CADe and a CADx scheme. Optional steps are indicated with dashed line

3. CADx schemes for MC clusters

3.1 Morphology-based CADx schemes

In the clinical practice the diagnosis of MC clusters is based on morphology (shape, size and intensity) properties and distribution properties of individual particles within a MC cluster, thus, most CADx schemes are also focused on the automated quantification of such properties (Cheng et al., 2003; Sampat et al., 2005; Costaridou et al., 2008; Elter & Horsch, 2009; Costaridou, 2011).

A number of authors have utilized a wide range of quantitative individual MC morphology properties (Patrick et al., 1991; Shen et al., 1994; Papadopoulos et al., 2008; Sklansky et al., 2000; Jiang et al., 1996). Specifically, size and shape features (area, perimeter, elongation, circularity, compactness, eccentricity, moment ratio, axis ratio, concavity index, effective thickness and volume as well as, shape signature) and MC intensity features (mean intensity, background intensity, contrast and edge strength) have been exploited.

CADx schemes that classify MC clusters are based on two categories of cluster features:

- Category I: Cluster features based on descriptive statistics (e.g. average, standard deviation, coefficient of variation, maximum, median, range) of individual MC morphology properties.
- Category II: Cluster features describing cluster morphology considering the cluster as an entire object (cluster area, diameter, perimeter, circularity, eccentricity, elongation, solidity and cluster background intensity). In this category the spatial distribution of individual MC particles within a cluster is also considered (number of MCs, structural index, proximity to the nearest MC, cluster density, as well as distance to pectoral and breast edge).

Table 1. summarizes morphology-based CADx schemes for MCs in terms of discriminant features (derived from Category I and/or Category II) including feature selection and classification techniques employed. Classification performance is also provided in terms of area under Receiver Operating Characteristic - ROC curve (A_z index) on patient and cluster-basis. Performance in patient-basis is derived by considering decision scores by both mammographic views (mediolateral oblique and craniocaudal). A disadvantage of these methods is that their performance is dependent on the accuracy of the segmentation method used. Specifically, the segmentation accuracy of less robust segmentation methods reduces the performance of morphology-based CADx schemes (Paquerault et al., 2004; Arikidis et al., 2008; Arikidis et al., 2009).

3.2 Texture-based CADx schemes

Another approach that overcomes limitations associated to segmentation issues is texture analysis applied on ROIs containing the MC cluster. This approach is based on the hypothesis that a malignancy (e.g. the MC) would cause changes in the texture of tissue surrounding it. Aiming at capturing such tissue texture alterations, CADx schemes have exploited various texture feature sets as well as feature selection and classification algorithms (Cheng et al., 2003; Sampat et al., 2005; Elter & Horsch, 2009), summarized in Table 2. Table 2 also provides classification performance of reported CADx schemes in a cluster-basis. Since a direct comparison of the reported CADx methodologies is not feasible, mainly due to the heterogeneous datasets analyzed, the attempted comparisons in the following paragraphs are only indicative of existing trends in texture analysis.

The grey level co-occurrence matrix (GLCM) characterizes the spatial distribution of grey levels in an image (Haralick et al., 1973). Features extracted from GLCMs provide information concerning image texture heterogeneity and coarseness, which is not necessarily visually perceived. The discriminating ability of GLCMs features, as extracted from original image ROIs containing MCs, has been demonstrated by most studies (Dhawan et al., 1996; Kocur et al., 1996; Kramer & Aghdasi 1999; Chan et al., 1997; Chan et al., 1998; Soltanian-Zadeh et al., 2004), with specific GLCMs feature combinations achieving an

Study	Discriminant Features	Feature selection/ Classification	Performance (A_z index)
Jiang, et al. 1996	^I Mean area and effective volume, Standard Deviation (SD) of effective thickness and effective volume, 2nd highest MC-shape-irregularity measure. ^{II} Number of MCs, circularity, area.	Qualitative correlation with radiologist's experience / Artificial Neural Network (ANN)	0.92 (patient) 0.83 (cluster)
Betal, et al. 1997	^I Percentage of irregular and round MCs, inter-quartile range of MC area. ^{II} Number of MCs.	Exhaustive search / k-nearest-neighbour	0.84 (patient)
Chan, et al. 1998	^I Coefficient of mean density variation, moment ratio variation and area variation, maximum moment ratio and area.	Genetic algorithm and stepwise discriminant analysis / Linear Discriminant Analysis (LDA)	0.79 (cluster)
Veldkamp, et al. 2000	^I SD of individual MC area, orientation and contrast, mean of individual MC area and orientation, cluster area. ^{II} Number of MCs, distance to pectoral edge and breast edge.	Sequential forward feature selection based on A_z value / k-nearest-neighbour	0.83 (patient) 0.73 (cluster)
Sklansky, et al. 2000	^I Mean area, aspect ratio and irregularity. ^{II} Number of MCs.	Genetic algorithm / ANN	0.75 (cluster)
Leichter, et al. 2000	^I Mean shape factor, SD of shape factor, brightness and area ^{II} Mean number of neighbours, mean distance to the nearest MC.	Stepwise discriminant analysis / LDA	0.98 (cluster)
Buchbinder, et al. 2002	^I Average of length extreme values.	Stepwise discriminant analysis / LDA	0.81 (cluster)
Paquerault, et al. 2004	^I Mean area and effective volume, relative SD of effective thickness and effective volume, 2nd highest MC-shape-irregularity. ^{II} Number of MCs, circularity, area.	Qualitative correlation with radiologist's experience / LDA and Bayesian ANN	0.86 (patient) 0.82 (cluster)
Arikidis, et al. 2008	^I SD of length extreme values.	Exhaustive search / LDA	0.86 (patient) 0.81 (cluster)

Table 1. Morphology-based CADx schemes for MC clusters

A_z of 0.88 in discriminating malignant from benign MC clusters (Chan et al., 1997). In addition, GLCMs feature have shown to be more effective than morphology-based features (Chan et al., 1998), while their combination can provide an even higher classification performance. Soltanian-Zadeh et al. (2004) demonstrated that GLCMs extracted from ROIs containing the MCs were superior to GLCMs extracted from segmented MCs and suggested that "there may be valuable texture information concerning the benignity or malignancy of the cluster in those areas that lie outside the MCs".

Aiming at capturing tissue texture alterations in multiscale representation, studies have also exploited first order statistics (FOS) (i.e. energy, entropy and square root of the coefficients norm) extracted from wavelet (Dhawan et al., 1996; Kocur et al., 1996; Soltanian-Zadeh et al., 2004) or multi-wavelet (Soltanian-Zadeh et al., 2004 transform subimages. Wavelet/

Study	Features	Feature selection / Classification	Performance ($A_z \pm SE$)
Dhawan et al., 1996	<ul style="list-style-type: none"> GLCMs features Entropy, Energy (wavelet packets; Daubechies 6/20) Cluster features 	Genetic Algorithm-based method / Backpropagation Neural Network, Linear classifier, k-Nearest Neighbor	Combined: 0.86±0.05 (cluster)
Kocur et al., 1996	<ul style="list-style-type: none"> SRN (DWT; \ Daubechies4 & Biorthogonal 9.7) GLCMs feature (angular second moment). Eigenimages (Karhunen-Loeve coefficients) 	ANN, Decision Boundary Analysis / Multilayer Perceptron Neural Network	Wavelet: 88%* (cluster)
Chan et al., 1997	<ul style="list-style-type: none"> GLCMs features 	Stepwise Discriminant Analysis / Artificial Neural Network	0.88 (cluster)
Chan et al., 1998	<ul style="list-style-type: none"> GLCMs features Cluster features (Morphological) 	Genetic Algorithm, Stepwise Discriminant Analysis / Linear Discriminant Analysis	Combined: 0.89±0.03 (cluster) 0.93±0.03 (patient)
Kramer & Aghdasi, 1999	<ul style="list-style-type: none"> GLCMs features Entropy, Energy (DWT; Daubechies 4/6/20 & Biorthogonal 2.8) Co-occurrence-based (DWT; Daubechies 4/6/20 & Biorthogonal 2.8) 	Sequential Forward Selection/ ANN, k-Nearest Neighbor	Combined: 94.8%* (cluster)
Soltanian-Zadeh et al., 2004	<ul style="list-style-type: none"> GLCMs features from segmented MCs and from ROIs containing the MCs Entropy, Energy (wavelet packets; Daubechies 6/10/12) Entropy, Energy (multi-wavelet, 3 Filters) Cluster features (shape) 	Genetic Algorithm / k-Nearest Neighbor	Multi-wavelet: 0.89 (cluster)
Karahaliou et al., 2008	<ul style="list-style-type: none"> First order statistics GLCMs features Laws' texture energy measures Energy, Entropy (redundant DWT; B-spline) Co-occurrence based (Decomposition: redundant DWT; Filter: B-spline; Levels: 1-3) 	Exhaustive search/ Probabilistic Neural Network	0.98±0.01 (cluster)

*Performance provided in % classification accuracy; GLCMs: Grey-level co-occurrence matrices; SRN: Square Root of the Norm of coefficients; DWT: Discrete Wavelet Transform.

Table 2. Texture-based CADx schemes for MC clusters

multiwavelet FOS have shown to be more effective than GLCMs features (Kocur et al., 1996; Soltanian-Zadeh et al., 2004) and shape features (Soltanian-Zadeh et al., 2004) suggesting the advantages offered by the multiscale representation of the tissue analyzed. Dhawan et al. (1996) demonstrated that the combination of GLCMs with FOS wavelet features, representing global and local texture respectively, is superior to cluster features; however, best performance was achieved by a selected feature set including GLCMs, wavelet and cluster features. An obvious extension of wavelet FOS is the computation of co-occurrence matrix features from wavelet decomposed subimages, to describe coefficients second order statistics (Van de Wouwer et al., 1998). Kramer and Aghdasi (1999) demonstrated that co-occurrence matrices features extracted from wavelet decomposed subimages were superior to GLCMs and wavelet FOS in discriminating malignant from benign MC clusters.

3.2.1 Texture analysis of the tissue surrounding MCs

As opposed to the previously described CADx approaches which analyze the texture pattern of ROIs containing the MC cluster, the MCs surrounding tissue analysis approach focuses on the investigation of the “net texture pattern” of the underlying breast tissue removing any bias induced by the presence of MCs.

The biological basis of the hypothesis is that as the tissue surrounding MCs is the one sampled and subjected to histopathological analysis to decide on benignity or malignancy, this tissue area should be subjected to texture analysis. The hypothesis was introduced by Thiele et al. (1996) who investigated texture properties of the tissue surrounding MCs on digital scout views acquired during the stereotactic biopsy procedure. The hypothesis was tested on a dataset of 54 cases (18 malignant/36 benign) exploiting GLCMs and fractal geometry based features and achieved a classification performance 85% (sensitivity 89%, specificity 83%) employing Linear and Logistic Discriminant analysis. Since its introduction on digital scout views, the feasibility of the MCs surrounding tissue analysis hypothesis has been further investigated on screening mammograms (Karahaliou et al., 2007a, 2007b, 2008).

In the following sections (4.1, 4.2 and 4.3) the potential contribution of this approach in CADx of MC clusters is investigated and compared to current state-of-the-art approaches, by means of a meta-analysis application paradigm of the sample analysed in (Karahaliou et al., 2007a, 2008; Arikidis et al., 2008).

4. Application paradigm

4.1 Texture vs. morphology analysis for MC cluster diagnosis

Methods performance inter-comparison is tested on a pilot dataset of 92 MC clusters. 49 MC clusters were malignant (as proven by biopsy) while 43 MC clusters were benign (either biopsy proven or without call-back). Mammograms were originated from the Digital Database for Screening Mammography (DDSM) (Heath et al., 2000) and correspond to digitization with a single laser scanner (LUMISIS) at a pixel depth of 12 bits and 50 μm pixel resolution. Mammograms correspond to extremely dense and heterogeneously dense breast parenchyma (density 3 and 4 according to ACR BIRADS lexicon). Figure 2 depicts the distribution of the 92 MC clusters with respect to malignancy assessment.

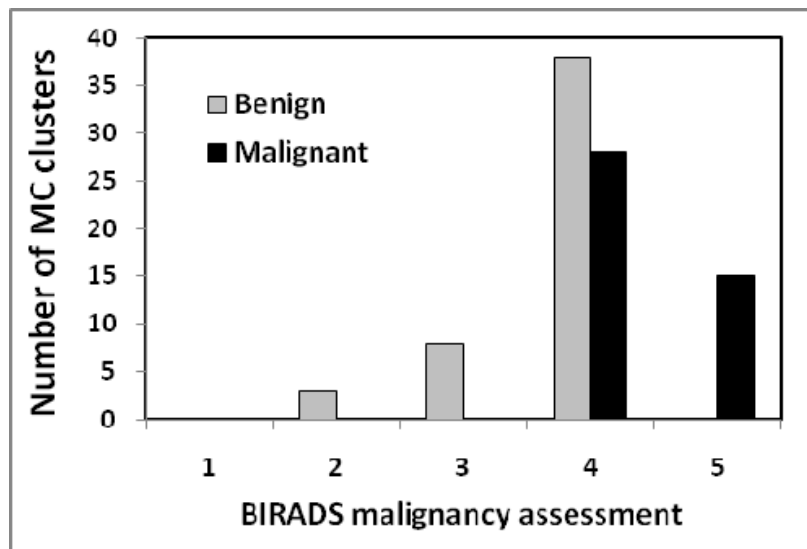


Fig. 2. Distribution of the dataset of 92 MC clusters with respect to malignancy rating provided in the DDSM. 1: negative, 2: benign, 3: probably benign, 4: suspicious abnormality, 5: highly suggestive of malignancy

a. Texture analysis of tissue surrounding MCs

The “MCs surrounding tissue” area is provided by MC segmentation and subsequent “exclusion” of the segmented MC areas from the ROI containing the cluster (Figure 3). As the approach requires only a “coarse” MC segmentation, requirements for accurate segmentation are relaxed, as compared to the corresponding ones of morphology-based CADx schemes. Wavelet based signatures (Van de Wouwer et al., 1998) were employed for quantification of the “net texture pattern” of the breast tissue. The specific texture feature category was selected due to its improved discriminating ability over three robust texture feature categories (first order statistics features (Gonzalez & Woods, 2000), Laws’ texture energy measures (Laws, 1979)) and grey level co-occurrence matrices (Haralick et al., 1973) previously adopted in CADx approaches for the differentiation of malignant from benign MC clusters.

Wavelet coefficient co-occurrence matrices (WCCMs) (Van de Wouwer et al., 1998) features were generated employing the redundant dyadic wavelet transform whose wavelet filter is the first-order derivative of a cubic B-spline (Mallat & Zhong, 1992). The transform was implemented using the ‘*algorithme `a trous`*’ (algorithm with holes), which does not involve down-sampling. The gradient magnitude coefficients of the 2nd and 3rd dyadic scale were considered for co-occurrence matrices feature extraction. Co-occurrence matrices were generated for 4 angles (0° , 45° , 90° , 135°) and for various displacement vector values d . From each co-occurrence matrix 16 features were extracted. For each d , the mean and range value of each feature over the four co-occurrence matrices were calculated. In order to define the “MCs surrounding tissue” area, wavelet decomposition was performed on original mammogram ROIs (513x513 pixels) containing the MC clusters. To deal with contaminated pixels adjacent to MC areas, the “coarsely” segmented MC areas were dilated in proportion to the filter lengths used to derive wavelet gradient magnitude coefficients. Figure 4 illustrates ST-ROIs on original mammogram and on gradient magnitude coefficients of the 2nd and 3rd dyadic scale of the wavelet transform employed.

The Stepwise Discriminant Analysis (SDA) was then employed to select one single feature subset from extracted WCCMs features. The selected subset referred here in as WCCMs*, is comprised of 3 WCCMs features corresponding to: Mean of Shade ($d=18$, scale 2), Range of Difference Variance ($d=14$, scale 3) and Mean of Information Measure of Correlation 1 ($d=18$, scale 3).

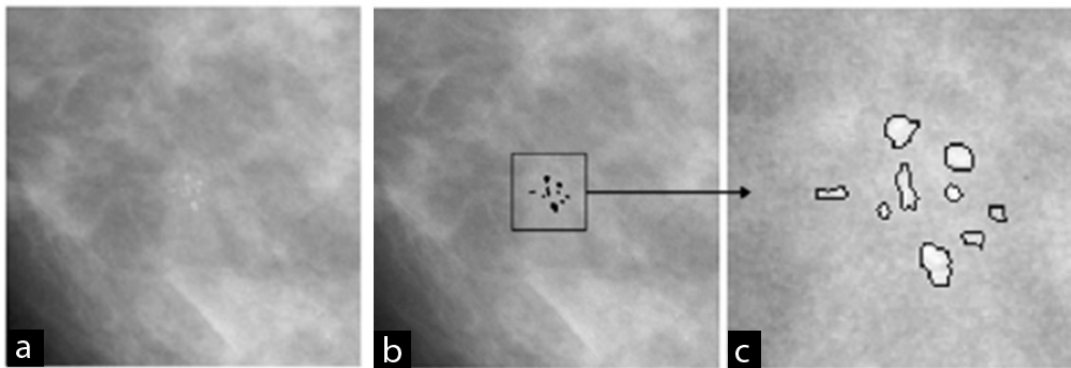


Fig. 3. Illustrative example of ST-ROI definition. (a) 513x513 pixel part of original mammogram containing a MC cluster (DDSM: volume cancer_09, case B_3406, RIGHT_CC). (b) Segmented MC areas (in black) of the cluster and 129x129 pixel ROI (black rectangle) containing the cluster. (c) Magnified ROI of figure (b). Surrounding tissue ROI (i.e. ST-ROI) corresponds to the area resulting from exclusion of segmented MC areas from the 129x129 pixel ROI. Borders of excluded MC areas are indicated with solid line

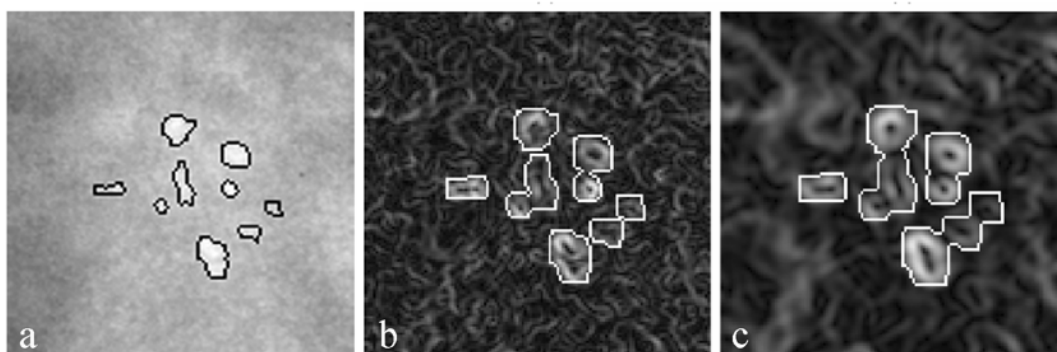


Fig. 4. ST-ROIs (129x129 pixels) on original (a) and wavelet gradient magnitude coefficients of the 2nd (b) and 3rd (c) dyadic scale. Borders of excluded MC areas are indicated with solid line

b. Texture analysis of ROIs containing the MCs

This approach is similar to the “MCs surrounding tissue” one with respect to texture feature extraction and classification without however requiring the “coarse” MC segmentation step. Specifically, 129x129 pixel ROIs centered at each cluster, identical to the ones employed in the “MC surrounding tissue” approach, were subjected to texture feature extraction by means of wavelet based signatures. The SDA was then employed to select one single feature subset. The selected subset referred here in as WCCMs**, is comprised of 4 WCCMs features corresponding to: Range of Inverse Difference Moment ($d=1$, scale 2), Mean of Difference Variance ($d=6$, scale 2), Range of Prominence ($d=6$, scale 2) and Mean of Contrast ($d=18$, scale 2).

c. Morphology analysis of MCs

A recently proposed segmentation algorithm was employed to segment individual MCs within each cluster, details of which can be found elsewhere (Arikidis et al., 2008). Briefly, the method is based on implementation of active rays on B-spline wavelet representation to identify MC contour point estimates in a coarse-to-fine strategy at two levels of analysis. An iterative region growing method is then used to delineate the final MC contour curve, with pixel aggregation constrained by the MC contour point estimates.

Ten (10) individual MC features were extracted from each segmented MC corresponding to: area, length, eccentricity, compactness, radial standard deviation, relative contrast, 2 regional moments (one related to the spread and one related to the eccentricity of object mass), one moment of region boundary and a shape roughness measure provided by Fourier descriptors. Twenty (20) MC cluster features were then generated by computing the mean and range of the above feature values over the entire cluster. The SDA was then employed to select one single feature subset from the 20 cluster features. The selected subset comprised of 3 cluster features corresponding to: mean of relative contrast, range of relative contrast and the regional moment related to object mass eccentricity.

The discriminating ability of the three selected feature subsets was investigated using a least squares minimum distance (LSMD) classifier, using the Leave-One-Out (LOO) (Theodoridis & Koutroumbas 1999) training-testing methodology. Classification performance of the three feature subsets (morphology, WCCMs* and WCCMs**) was evaluated by means of the A_z index (area under ROC curve).

The morphology-based feature subset achieved an $A_z \pm$ standard error (SE) of 0.809 ± 0.046 with lower and upper 95% Confidence Interval (CI) values of 0.698 and 0.882, respectively. On the same dataset (of 92 MC clusters) the "MCs surrounding tissue texture analysis" approach achieved $A_z \pm$ SE of 0.882 ± 0.036 (95% CI values: 0.788, 0.936) employing the WCCMs* subset. The commonly adopted approach of analysing tissue ROIs containing the MCs achieved $A_z \pm$ SE of 0.803 ± 0.048 (95% CI values: 0.688, 0.879) employing the WCCMs** subset. ROC curves corresponding to the three feature subsets are provided in Fig. 5. Table 3 provides classification performance comparison among the three selected feature subsets.

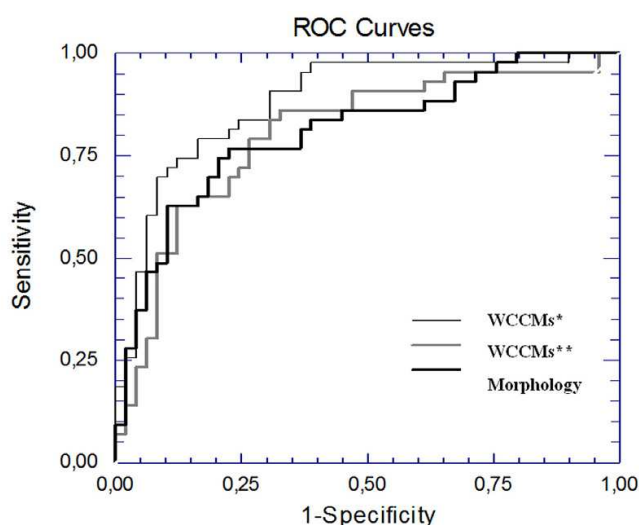


Fig. 5. ROC curves corresponding to the morphology, the WCCMs* (MCs surrounding tissue) and the WCCMs** (tissue containing the MCs) selected feature subsets

	$A_z \pm SE$	p-value
Morphology vs. WCCMs*	0.809±0.046 vs. 0.881±0.036	0.15
Morphology vs. WCCMs**	0.809±0.046 vs. 0.803±0.048	0.92
WCCMs* vs. WCCMs**	0.881±0.036 vs. 0.803±0.048	0.11

Table 3. p-values (z-test) for classification performance comparison among selected subsets from the three approaches

4.2 Texture plus morphology analysis for MC cluster diagnosis

In order to investigate the combined performance of texture- and morphology-based analysis two additional feature sets were generated by (a) merging the morphology-based selected subset with the WCCMs* subset and (b) merging the morphology-based selected subset with the WCCMs** subset.

From each merged feature set one subset was generated by means of an exhaustive search procedure. Specifically, the LSMD classifier was designed with all possible feature combinations, from 2 up to 6 features, and for each combination the classifier performance was evaluated by means of the LOO training-testing methodology. The feature combination with the highest classification performance (by means of A_z index) and the minimum number of features was selected.

Table 4 summarizes classification performance of the two selected subsets by means of $A_z \pm SE$ and 95% asymmetric CI values. No statistically significant difference was observed in classification performance of the two approaches ($p > 0.05$).

	Features included in subset	$A_z \pm SE$	[Lower, Upper] 95% asymmetric CI
Morphology and WCCMs*	Regional Moment (eccentricity)	0.899±0.035	[0.802, 0.950]
	Mean of Shade ($d=18$, scale 2)		
	Range of Difference Variance ($d=14$, scale 3)		
	Mean of Information Measure of Correlation 1 ($d=18$, scale 3)		
Morphology and WCCMs**	Mean of Relative Contrast	0.868±0.038	[0.771, 0.926]
	Range of Relative Contrast		
	Regional Moment (eccentricity)		
	Mean of Difference Variance ($d=6$, scale 2)		
	Mean of Contrast ($d=18$, scale 2)		

Table 4. Classification performance of the two combined (texture and morphology) selected subsets by means $A_z \pm SE$ and 95% asymmetric Confidence Interval (CI) values. WCCMs*: selected texture feature subset employing the “MCs surrounding tissue” approach. WCCMs**: selected texture feature subset employing the commonly adopted approach of analysing tissue ROIs containing the MCs

4.3 Discussion

Texture analysis is ultimately concerned with automated methods that can derive image information from a purely computational point of view. As such, is nothing than numeric manipulation of digital or digitized images to get quantitative measurements (Tourassi, 1999). However, in contrast to morphology analysis, texture analysis can potentially improve decision making by capturing clues “beyond the human eye”. Morphology analysis based schemes quantify visually perceived properties, mimicking radiologist decision making in an objective and reproducible way. Texture analysis has a divergent role when considered in decision making. It can mimic radiologist perception of image texture (when texture differences are visually perceived) or it can augment the visual skills of the radiologists by extracting/quantifying image features that may be relevant to the diagnostic problem, but are not visually extractable.

In case of CADx schemes based on morphology analysis of MCs the first approach is applicable. Specifically, image analysis approaches are employed to quantify individual MCs properties that are commonly assessed by the radiologist to provide a final decision concerning diagnosis and patient management. In case of CADx schemes based on texture analysis of ROIs including MCs the second approach is applicable. Specifically, image analysis approaches are employed to quantify the texture properties of ROIs, e.g. to capture the increased heterogeneity, due to presence of large number of MCs within ROI, but also capture texture alterations of tissue surrounding MCs. The first is visually perceived, and in a sense is also one of the diagnostic criteria adopted in clinical practice for MCs. The second (i.e. the MCs surrounding tissue heterogeneity) is not currently evaluated in the clinical practice but accounts for an approach worthy of being further exploited.

Nonetheless, texture analysis is not a panacea for the diagnostic interpretation of radiographic images. As the pursuit of texture analysis is based on the hypothesis that the texture signature of an image is relevant to the diagnostic task at hand, the hypothesis should always be tested (Tourassi, 1999).

In the current application paradigm, we tested the hypothesis that wavelet texture signatures of tissue surrounding MCs as depicted on screening mammograms is relevant to the diagnostic task. Results have demonstrated the feasibility of the “MCs surrounding tissue” texture analysis approach in the differentiation of malignant from benign MC clusters on screening mammograms, in support of the hypothesis originally formulated by (Thiele et al., 1996) on stereotactic scout views. While a direct comparison with the results of this study (Thiele et al., 1996) is not feasible, due to the different nature of the datasets analyzed, comparable performance is achieved.

As compared to other texture-based CADx schemes analyzing ROIs containing the cluster (Dhawan et al., 1996; Kocur et al., 1996; Chan et al., 1997; Chan et al., 1998; Kramer & Aghdasi 1999; Soltanian-Zadeh et al., 2004), the performance achieved by the wavelet texture signatures, employing the MCs surrounding tissue approach, is also comparable. However, heterogeneity of the datasets analyzed renders direct comparison not feasible.

As compared to the morphology-based CADx schemes, the “MCs surrounding tissue” texture analysis approach has the advantage of relaxing segmentation accuracy requirements. However, the current study demonstrated the advantages of combining wavelet texture signatures derived from the tissue surrounding MCs with morphology

features of MC clusters, in accordance to Chan et al. (1998) who combined GLCMs features (from ROIs containing the cluster) with morphology-based ones.

While no statistically significant difference between the two texture-based approaches was observed, the results of this study demonstrate a trend in favour of the “MCs surrounding tissue” texture analysis approach over the commonly adopted one of analysing ROIs containing the MCs. We attribute this trend to the fact that the “MCs surrounding tissue texture analysis” allows an investigation of the net texture pattern of the underlying tissue, which is the one that generates the MCs, removing bias due to the number and distribution of MCs within the depicted tissue.

Additional research efforts are required for validating/establishing the computer-extracted image features (morphology-based or texture-based) of MC clusters as diagnostic image-based biomarkers for breast cancer. Specifically, research should be focused on investigating the relationship between quantitatively extracted features and histopathological indices.

5. Migration to computer-aided prognosis

Computer-aided diagnosis of mammographic MCs has also been extended from the task of differentiating malignant from benign MC clusters to prognostic tasks towards the identification of potential mammographic image-based prognostic markers.

Specifically, morphology-based analysis of MC clusters applied on magnification mammograms has been exploited for the classification of 58 MC clusters into fibroadenoma, mastopathy, noninvasive carcinoma of the noncomedo type, noninvasive carcinoma of the comedo type and invasive carcinoma (Nakayama et al., 2004). Features considered are (i) the variation in the size of microcalcifications within a cluster, (ii) the variation in pixel values of microcalcifications within a cluster, (iii) the shape irregularity of microcalcifications within a cluster, (iv) the extent of the linear and branching distribution of microcalcifications, and (v) the distribution of microcalcifications in the direction toward the nipple. The Bayes decision rule was employed for distinguishing between five histological categories demonstrating promising results.

The potential contribution of follow-up mammograms in this specific prognostic task (i.e. in identifying the histological classification of clustered MCs) was also evaluated (Nakayama et al., 2006). Specifically, the previously defined five morphology features were extracted from previous and current magnification mammograms. The ten features were merged by means of a Modified Bayes discriminant function for the histological classification of 93 MC clusters (55 malignant and 38 benign).

Classification results were improved by employing a nearest neighbor criterion and by augmenting the feature set (i.e. adding the number of microcalcifications within the cluster) (Nakayama et al., 2007).

The identification of potential image-based prognostic markers for breast cancer, i.e. quantitative image features capable of predicting biological behaviour and disease aggressiveness, accounts for an emerging research area, expected to have a significant impact on patient management and treatment response assessment.

6. Conclusions

Only a few research efforts (Chan et al., 1998; Soltanian-Zadeh et al., 2004) have focused on comparing state-of-the-art approaches for computer-aided diagnosis of breast cancer, including the presented application paradigm which considered a pilot dataset. Thus, the systematic evaluation of proposed methods performance utilizing large and publicly available datasets is a necessity. Furthermore, method inter-comparison should consider testing on datasets generated by multicenter studies to ensure a large size, inclusion of varying case subsets with respect to lesion types (e.g. MCs of varying morphology and distribution) and image acquisition systems (i.e. digitized vs. FFDM).

It is important to investigate the effect of reported CADx schemes on radiologist performance in breast cancer diagnosis task, by considering a radiologist's diagnosis task aided by a specific CADx scheme and an un-aided corresponding one, also taking into account issues related to interaction of radiologist with a CADx scheme. The contribution of CADx schemes in reducing intra- and inter-observer variability should also be investigated.

Advances in breast imaging have broadened the role of computer-based approaches in breast cancer diagnosis further suggesting multimodality and multi-parametric approaches. Multi-modality CADx schemes that combine features extracted from different imaging modalities, each one capturing additional tissue properties, may be advantageous to single-modality CADx in the task of differentiating between malignant and benign lesions (Yuan et al., 2010), especially in the case of benign and malignant lesions with overlapping imaging features on a single imaging modality. Finally, the multi-modality approach has an increased potential towards identification of potential new diagnostic and prognostic biomarkers for breast cancer.

7. Acknowledgments

Part of this work is supported by the Caratheodory Programme (C.183) of the University of Patras, Greece.

8. References

- American College of Radiology (ACR) Breast Imaging Reporting and Data System Atlas (BI-RADS Atlas): Mammography, Ultrasound, and Magnetic Resonance Imaging, 4th ed. Reston, VA: ACR, 2003
- Arikidis, N.S.; Skiadopoulos, S.; Karahaliou, A.; Likaki, E.; Panayiotakis, G.; & Costaridou, L. (2008). B-spline active rays segmentation of microcalcifications in mammography. *Medical Physics*, Vol. 3, No. 11, (November 2008), pp. 5161-5171, ISSN 0094-2405
- Arikidis, N.; Karahaliou, A.; Skiadopoulos, S.; Likaki, E.; Panayiotakis, G.; & Costaridou, L.(2009). Integrating multiscale polar active contours and region growing for microcalcifications segmentation in mammography. *Journal of Instrumentation*, JINST 4, P07009, (July 2009), pp. 12-16, ISSN 1748-0221

- Baker, J.A.; Kornguth, P.J & Floyd, C.E. (1996). Breast imaging reporting and data system standardized mammography lexicon: observer variability in lesion description. *American Journal of Roentgenology*, Vol. 166, No. 4, (April 1996), pp. 773-778, ISSN 0361-803X
- Bassett, L.W. (2000). Digital and Computer-Aided Mammography. *The Breast Journal*, Vol. 6, No. 5, pp. 291-293, ISSN 1075-122X
- Betal, D.; Roberts, N. & Whitehouse, G.H. (1997). Segmentation and numerical analysis of microcalcifications on mammograms using mathematical morphology. *The British Journal of Radiology*, Vol. 70, No. 837, (September 1997), pp. 903-917, ISSN 0007-1285
- Buchbinder, S.S.; Leichter, I.; Lederman, R.; Novak, B.; Bamberger, P.; Coopersmith, H. & Fields, S.I. (2002). Can the size of microcalcifications predict malignancy of clusters at mammography? *Academic Radiology*, Vol. 9, No.1, (January 2002), pp. 18-25, ISSN 1076-6332
- Chan, H.P.; Sahiner, B.; Petrick, N.; Helvie, M.A.; Lam, K.L.; Adler, D.D. & Goodsitt, M.M. (1997). Computerized classification of malignant and benign microcalcifications on mammograms: Texture analysis using an artificial neural network. *Physics in Medicine and Biology*, Vol. 42, No. 3, pp. 549-567, ISSN 0031-9155
- Chan, H.P.; Sahiner, B.; Lam, K.L.; Petrick, N.; Helvie, M.A.; Goodsitt, M. & Addler D.D. (1998). Computerized analysis of mammographic microcalcifications in morphological and texture feature spaces. *Medical Physics*, Vol. 25, No. 10, (October 1998), pp. 2007-2019, ISSN 0094-2405
- Chan, H.P.; Sahiner, B.; Petrick, N.; Hadjiiski, L.; Paquerault, S. (2005). Computer-Aided Diagnosis of Breast Cancer. In: *Medical Image Analysis Methods*, Costaridou, L. (Ed.), CRC Press, Taylor & Francis Group, ISBN 0-8493-2089-5, Boca Raton, FL, US
- Cheng, H.D.; Cai, X.; Chen, X.; Hu, L.; Lou, X. (2003). Computer-aided detection and classification of microcalcifications in mammograms: a survey. *Pattern Recognition*, Vol. 36, No. 12, (December 2003), pp.2967-2991, ISSN 0031-3203
- Cole, E.B.; Pisano, E.D.; Kistner, E.O.; Muller, K.E.; Brown, M.E.; Feig, S.A. et al. (2003). Diagnostic Accuracy of Digital Mammography in Patients with Dense Breasts Who Underwent Problem-solving Mammography: Effects of Image Processing and Lesion Type. *Radiology*, Vol. 226, (January 2003),pp.153-160, ISSN 0033-8419
- Costaridou, L.; Skiadopoulos, S.; Karahaliou, A.; Arikidis, N.; Panayiotakis, G. (2008). Computer-Aided Diagnosis in Breast Imaging: Trends and Challenges, In: *Handbook of Research on Advanced Techniques in Diagnostic Imaging and Biomedical Applications*. Exarchos, T.P.; Papadopoulos, A. & Fotiadis, D .I. (Eds), IGI Global., ISBN 9781605663142
- Costaridou, L. (2011). CADx Mammography. In: *Biomedical Image Processing, Biological and Medical Physics*, Biomedical Engineering, T.M. Deserno (Ed.), Springer-Verlag, ISBN 978-3-642-15815-5, Berlin Heidelberg

- Dhawan, A.P.; Chitre, Y.; Kaiser-Bonasso, C. (2000) Analysis of mammographic microcalcifications using gray-level image structure features. *IEEE Transactions on Medical Imaging*, Vol. 15, No. 3, (June 1996), pp. 246–259, ISSN 0278-0062
- Duncan, J.S. & Ayache, N. (2000). Medical Image Analysis: Progress over two decades and the challenges ahead. *IEEE Transactions on Pattern Analysis and Machine Intelligence*, Vol. 22, No. 1, (January 2000), pp. 85-106, ISSN 0162-8828
- Elter, M. & Horsch, A. (2009). CADx of mammographic masses and clustered microcalcifications: A review. *Medical Physics*; Vol. 36, No. 6, (June 2009), pp. 2052-2068, ISSN 0094-2405
- Fenton, J.J.; Taplin, S.H.; Carney, P.A.; Abraham, A.; Sickles, E.A.; D’Orsi, C.B. et al. (2007). Influence of computer-aided detection on performance of screening mammography. *The New England Journal of Medicine*, Vol. 356, No. 14, (April 2007), pp. 1399-1409, ISSN 0028-4793
- Giger, M.L.; Chan, H.P. & Boone, J. (2008). Anniversary paper: History and status of CAD and quantitative image analysis: the role of Medical Physics and AAPM. *Medical Physics*, Vol. 35, No. 12, (November 2008), pp. 5799-5820, ISSN 0094-2405
- Gonzalez, R.C. & Woods, R.E. (Eds). (2002). *Digital image processing*, Prentice-Hall, Inc., ISBN: 0201180758, New Jersey, USA
- Gur, D.; Sumkin, J.H.; Rockette, H.E.; Ganott, M.; Hakim, C.; Hardesty, L.; Poller, W.R.; Shah, R. & Wallace, L. (2004). Changes in breast cancer detection and mammography recall rates after the introduction of a computer-aided detection system. *Journal of the National Cancer Institute*, Vol. 96, No. 3, (February 2004), pp.185-190, ISSN 0027-8874
- Haralick, R.M.; Shanmugam, K. & Dinstein, I. (1973). Textural features for image classification. *IEEE Transactions on Systems Man and Cybernetics*, Vol. SMC-3, No. 6, (November 1973), pp. 610-621, ISSN 0018-9472
- Heath, M.; Bowyer, K.; Kopans, D.; Moore, R. & Kegelmeyer, P. (2000). The Digital Database for Screening Mammography. *Proceedings of the 5th International Workshop on Digital Mammography, IWDM*, ISBN, Toronto, Canada, June 11–14, 2000
- Jiang, Y.; Nishikawa, R.M.; Wolverton, D.E.; Metz, C.E.; Giger, M.L.; Schmidt, R.A. et al. (1996). Malignant and benign clustered microcalcifications: automated feature analysis and classification. *Radiology*, Vol. 198, No. 3, (March 1996), pp. 671-678, ISSN 0033-8419
- Karahaliou, A.; Boniatis, I.; Sakellaropoulos, P.; Skiadopoulos, S.; Panayiotakis, G. & Costaridou, L. (2007a). Can texture of tissue surrounding microcalcifications in mammography be used for breast cancer diagnosis. *Nuclear Instruments and Methods in Physics Research A*, Vol. 580, No. 2, (June 2007), pp. 1071-1074, ISSN 0168-9002
- Karahaliou, A.; Skiadopoulos, S.; Boniatis, I.; Sakellaropoulos, P.; Likaki, E.; Panayiotakis, G. & Costaridou, L. (2007b). Texture analysis of tissue surrounding microcalcifications on mammograms for breast cancer diagnosis. *The British Journal of Radiology*, Vol. 80, No. 956, (August 2007), pp. 648-656, ISSN 0007-1285

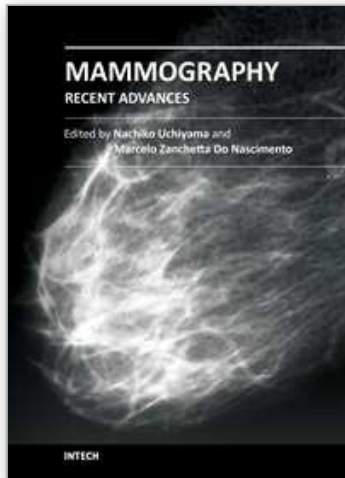
- Karahaliou, A.; Boniatis, I.; Skiadopoulou, S.; Sakellaropoulos, P.; Arikidis, N.; Likaki, E.; Panayiotakis, G. & Costaridou, L. (2008). Breast cancer diagnosis: Analyzing texture of tissue surrounding microcalcifications. *IEEE Transactions on Information Technology in Biomedicine*, Vol. 12, No. 6, (November 2008), pp. 731-738, ISSN 1089-7771
- Kocur, C.M.; Rogers, S.K.; Myers, L.R.; Burns, T.; Kabrisky, M.; Hoffmeister, J.W. et al. (1996). Using neural networks to select wavelet features for breast cancer diagnosis. *IEEE Engineering in Medicine and Biology*, Vol. 15, No. 3, pp. 95-102, ISSN 0739-5175
- Kopans, DB. (Ed.). (2007). *Breast Imaging*, 3rd Edition, Lippincott Williams & Wilkins, ISBN/ISSN: 9780781747684, Baltimore, MD
- Kramer, D. & Aghdasi, F. (1999). Texture analysis techniques for the classification of microcalcifications in digitized mammograms. *Proceedings of the 5th IEEE AFRICON Conference Electrotechnical Service for Africa*, ISBN 0780355466, Cape Town, South Africa, September - October 1999
- Laws, K.I. (1979). Texture energy measures. *Proceedings of DARPA Image Understanding Workshop*, Los Angeles, November 1979
- Leichter, I.; Lederman, R.; Bamberger, P.; Novak, B.; Fields, S. & Buchbinder, S.S. (1999). The use of an interactive software program for quantitative characterization of microcalcifications on digitized film-screen mammograms. *Investigative Radiology*, Vol. 34, No. 6, pp. 394-400, ISSN 1536-0210
- Mallat, S. & Zhong, S. (1992). Characterisation of signals from multiscale edges. *IEEE Transactions in Pattern Analysis and Machine Intelligence*, Vol. 14, No. 7, (July 1992), pp. 710-732, ISSN 0162-8828
- Markey, M.K.; Lo, J.Y.; Floyd, C.E.; (2002). Differences between computer-aided diagnosis of breast masses and that of calcifications. *Radiology*, Vol. 223, No. 2, (May 2002), pp. 489-493, ISSN 0033-8419
- Nakayama, R.; Uchiyama, Y.; Watanabe, R.; Katsuragawa, S.; Namba, K. & Doi, K. (2004). Computer-aided diagnosis scheme for histological classification of clustered microcalcifications on magnification mammograms. *Medical Physics*, Vol. 31, No. 4, (April 2004), pp. 789-799, ISSN 0094-2405
- Nakayama, R.; Watanabe, R.; Namba, K.; Takeda, K.; Yamamoto, K.; Katsuragawa, S. & Doi, K. (2006). Computer-aided diagnosis scheme for identifying histological classification of clustered microcalcifications by use of follow-up magnification mammograms. *Academic Radiology*, Vol. 13, No. 10, (October 2006), pp. 1219-1228, ISSN 1076-6332
- Nakayama, R.; Watanabe, R.; Namba, K.; Takeda, K.; Yamamoto, K.; Katsuragawa, S. & Doi, K. (2007). An improved computer-aided diagnosis scheme using the nearest neighbor criterion for determining histological classification of clustered microcalcifications. *Methods of Information in Medicine*, Vol. 46, No. 6, pp. 716-722, ISSN 0026-1270
- Papadopoulos, A.; Fotiadis, D.I. & Likas, A. (2005). Characterization of clustered microcalcifications in digitized mammograms using neural networks and support vector machines. *Artificial Intelligence in Medicine*, Vol.34, No.2, (June 2005), pp. 141-150, ISSN 0933-3657

- Papadopoulos, A.; Fotiadis, D.I & Costaridou, L. (2008). Improvement of microcalcification cluster detection in mammography utilizing image enhancement techniques. *Computers in Biology & Medicine*, Vol. 38, No. 10, (October 2008), pp. 1045-1055, ISSN 0010-4825
- Paquerault, S.; Yarusso, L.M.; Papaioannou, J.; Jiang, Y.; Nishikawa, R.M. (2004). Radial gradient-based segmentation of mammographic microcalcifications: observer evaluation and effect on CAD performance. *Medical Physics*, Vol.31, No. 9, (September 2004), pp. 2648-2657, ISSN 0094-2405
- Patrick, E.A.; Moskowitz, M.; Mansukhani, V.T.; Gruenstein, E.I. (1991). Expert learning system network for diagnosis of breast calcifications. *Investigative Radiology*, Vol. 26, No. 6, (June 1991), pp. 534-539, ISSN 1536-0210
- Pisano, E.D. (2000). Current status of full-field digital mammography. *Radiology*, Vol. 214, No. 1, (January 214), pp. 26-28, ISSN 0033-8419
- Sampat, P.M.; Markey, M.K. & Bovik, A.C. (2005). Computer-aided detection and diagnosis in mammography. In: *Handbook of image and video processing*. Bovik, A.C. (Ed.). pp. 1195-1217, Academic Press, ISBN 0121197921, New York
- Shen, L.; Rangayyan, R.M. & Desautels, J.E.L. (1994). Application of shape analysis to mammographic calcifications. *IEEE Transactions on Medical Imaging*, Vol. 13, No. 2, (June 1994), 263-274, ISSN 0278-0062
- Skaane, P.; Diekmann, F.; Balleyguier, C.; Diekmann, S.; Piguët, J.C.; Young, K.; Abdelnoor, M. & Niklason, L. (2008). Observer variability in screen-film mammography versus full-field digital mammography with soft-copy reading. *European Radiology*, Vol. 18, No. 6, (June 2008), pp. 1134-1143, ISSN 0938-7994
- Sklansky, J.; Tao, E.Y.; Bazargan, M.; Ornes, C.J.; Murchinson, R.C. & Teklehaimanot, S. (2000). Computer-aided, case-based diagnosis of mammographic regions of interest containing microcalcifications. *Academic Radiology*, Vol. 7, No. 6, (June 2000), pp. 395-405, ISSN 1076-6332
- Soltanian-Zadeh, H.; Rafee-Rad, F. & Pourabdollah-Nejad, D. (2004). Comparison of multiwavelet, wavelet, Haralick, and shape features for microcalcification classification in mammograms. *Pattern Recognition*, Vol. 37, pp. 1973-1986, ISSN 0031-3203
- Theodoridis, S. & Koutroumbas, K. (Eds.). (1999). *Pattern recognition*. Academic Press, New York
- Thiele, D.L.; Kimme-Smith, C.; Johnson, T.D.; McCombs, M. & Bassett, L.W. (1996). Using tissue texture surrounding calcification clusters to predict benign vs malignant outcomes. *Medical Physics*, Vol. 23, No. 4, (April 1996), pp. 549-555, ISSN 0094-2405
- Tourassi, G.T. (1999). Journey toward computer-aided diagnosis: role of image texture analysis. *Radiology*, Vol. 213, No. 2, (November 1999), pp. 317-320, ISSN 0033-8419
- Yuan, Y.; Giger, M.L.; Li, H.; Bhooshan, N. & Sennett, C.A. (2010). Multimodality Computer-Aided Breast Cancer Diagnosis with FFDM and DCE-MRI. *Academic Radiology*, Vol. 17, No. 9, (September 2010), pp. 1158-1167, ISSN 1076-6332

- Van de Wouwer, G.; Scheunders, P. & Van Dyck, D. (1999). Statistical texture characterization from discrete wavelet representations. *IEEE Transactions on Image Processing*, Vol. 8, No. 4, pp. 592-598, ISSN 1057-7149
- Veldkamp, W.J.H.; Karssemeijer, N.; Otten, J.D.M. & Hendriks, J.H.C.L. (2000). Automated classification of clustered microcalcifications into malignant and benign types. *Medical Physics*, Vol. 27, No. 11, (November 2000), pp. 2600-2608, ISSN 0094-2405

IntechOpen

IntechOpen



Mammography - Recent Advances

Edited by Dr. Nachiko Uchiyama

ISBN 978-953-51-0285-4

Hard cover, 418 pages

Publisher InTech

Published online 16, March, 2012

Published in print edition March, 2012

In this volume, the topics are constructed from a variety of contents: the bases of mammography systems, optimization of screening mammography with reference to evidence-based research, new technologies of image acquisition and its surrounding systems, and case reports with reference to up-to-date multimodality images of breast cancer. Mammography has been lagged in the transition to digital imaging systems because of the necessity of high resolution for diagnosis. However, in the past ten years, technical improvement has resolved the difficulties and boosted new diagnostic systems. We hope that the reader will learn the essentials of mammography and will be forward-looking for the new technologies. We want to express our sincere gratitude and appreciation to all the co-authors who have contributed their work to this volume.

How to reference

In order to correctly reference this scholarly work, feel free to copy and paste the following:

Anna N. Karahaliou, Nikolaos S. Arikidis, Spyros G. Skiadopoulos, George S. Panayiotakis and Lena I. Costaridou (2012). Computerized Image Analysis of Mammographic Microcalcifications: Diagnosis and Prognosis, Mammography - Recent Advances, Dr. Nachiko Uchiyama (Ed.), ISBN: 978-953-51-0285-4, InTech, Available from: <http://www.intechopen.com/books/mammography-recent-advances/computerized-image-analysis-of-mammographic-microcalcifications-diagnosis-and-prognosis>

INTECH
open science | open minds

InTech Europe

University Campus STeP Ri
Slavka Krautzeka 83/A
51000 Rijeka, Croatia
Phone: +385 (51) 770 447
Fax: +385 (51) 686 166
www.intechopen.com

InTech China

Unit 405, Office Block, Hotel Equatorial Shanghai
No.65, Yan An Road (West), Shanghai, 200040, China
中国上海市延安西路65号上海国际贵都大饭店办公楼405单元
Phone: +86-21-62489820
Fax: +86-21-62489821

© 2012 The Author(s). Licensee IntechOpen. This is an open access article distributed under the terms of the [Creative Commons Attribution 3.0 License](#), which permits unrestricted use, distribution, and reproduction in any medium, provided the original work is properly cited.

IntechOpen

IntechOpen